Original Research

Curcumin derivative 1, 2-bis [(3E, 5E)-3, 5-bis [(2-chlorophenyl) methylene]-4-oxo-1-piperidyl] ethane-1, 2-dione (ST03) induces mitochondria mediated apoptosis in ovarian cancer cells and inhibits tumor progression in EAC mouse model

Jinsha Koroth [a,b], Raghunandan Mahadeva [a], Febina Ravindran [a], Tanvi R Parashar [a], Vinay Teja [a], Subhas S Karki [c], Bibha Choudhary [a,*]

[a] *Institute of Bioinformatics and Applied Biotechnology, Electronic city phase 1, Bangalore 560100, Karnataka, India*
[b] *Manipal Academy of Higher Education, Manipal 576104, India*
[c] *Department of Pharmaceutical Chemistry, KLE Academy of Higher Education and Research, KLE College of Pharmacy, Rajajinagar, Bangalore, KN, India*

ARTICLE INFO

ABSTRACT

Curcumin is known for its anticancer properties, but its clinical application is limited due to its poor bioavailability and chemical stability. In this study we report the curcumin derivative, ST03 (1,2-bis[(3E,5E)-3,5-bis[(2-chlorophenyl)methylene]-4-oxo-1-piperidyl]ethane-1,2-dione) exhibits ∼ 14 fold better bioavailability compared to curcumin and is detectable in plasma up to 12 h. ST03 induces ROS, activates the intrinsic apoptotic pathway as evident by disruption of mitochondrial membrane potential, and induction of proapoptotic proteins in ovarian cancer lines PA1 and A2780. ST03 also blocked the migration of ovarian cancer cells. ST03 exerted its antitumor effect in-vivo in the EAC mouse model by activating the intrinsic apoptotic pathway. Our findings demonstrate ST03, a curcumin derivative, with better bioavailability and stability with no discernable toxicity in vivo to be a promising drug candidate for anticancer therapies.

Introduction

Cancer is a deadly disease on the rise, with implications on the economy. Although there are few success stories in cancer treatment owing to early detection and improved treatment modalities, complete elimination of cancer is a challenge. Hence, there is a univocal urge to develop an effective anticancer agent/treatment.

Compounds from natural sources such as phytochemicals have gained popularity for cancer treatment due to their multimodal activity and minimal systemic toxicity [39,54,61]. Curcumin is one such phytochemical studied extensively for its therapeutic activity and least toxicity [3]. It is a broad spectrum drug with a curative effect on diseases like cancer and Alzheimer's, cystic fibrosis, arthritis, other systemic disorders, and infectious diseases [1,2,17,23,27,38,40,44]. Curcumin targets multiple cellular pathways leading to cell death in cancer cells [52,68]. However, due to its low potency, bioavailability, and stability,

its clinical utility is limited [4,10,32]. To overcome this, several curcumin derivatives and formulations have been developed to enhance bioavailability and stability [14,60].

Curcumin and curcumin derivatives have been shown to induce reactive oxygen species (ROS) in several cancer cell lines [51,34]. High levels of ROS have been shown to alter proteins, lipids and generate breaks in DNA leading to cell death [46,58]. ROS is known to regulate p53 and activate apoptosis [26]. In mitochondria, the complex I, complex III and complex IV of ETC have been shown to be involved in generation of ROS [66]. The mitochondria codes for 13 proteins which are part of the OXPHOS complex [15]. Mutations in these genes have been associated with tumour progression [65]. In general, if ROS levels exceed a certain threshold, they will impair OXPHOS complexes and further stimulate ROS production. Chemotherapeutic drugs are reported to act via induction of ROS [63].

We have developed a series of 1, 2-bis [(3E, 5E)−3, 5-dibenzylidene-

---

4-oxo-1-piperidyl] ethane-1, 2-dione derivatives derived from the parent compound curcumin and tested it on various cancer cell lines [30]. We observed these compounds (in nM range) were ~100 times potent than curcumin (~10 μM range). Previous studies have reported that these 1,2-bis[(3E,5E)−3,5-dibenzylidene-4-oxo-1-piperidyl] ethane-1,2-dione derivatives are broad-spectrum anti-cancer compounds exerting anti-cancer activity in multiple cancer cell lines [12, 50]. In the present study, we report that ST03 has better bioavailability and stability than curcumin. ST03 induces ROS, intrinsic apoptotic pathway, and inhibits migration in ovarian cancer cell lines. Further, we also demonstrate that the compound can reduce tumor growth in EAC tumor-bearing mice models without toxicity.

Materials and methods

In-vitro studies

Cell lines and cultures

PA1 (Ovarian Teratocarcinoma origin) and A2780 (Ovarian epithelial origin) cell lines were purchased from NCCS (Pune, India) and ATCC (Manassas, VA, USA) respectively. PA1 cells were cultured in MEM (GIBCO, Lonza) containing 10% FBS (GIBCO, South America origin), 1X Antibiotic-Antimycotic (GIBCO) and 1X MEM NEA (GIBCO); A2780 cell lines were cultured in RPMI-1640 supplemented with 10% FBS (GIBCO, South America origin) and 1X Antibiotic-Antimycotic (GIBCO); all the cell lines were maintained at 37°C with 5% CO2 in a humidified incubator.

Chemicals and reagents

The study used reagents and chemicals purchased from MP Biomedicals, USA; Antibodies from Cell signaling technology, Santa Cruz Biotechnology, and Biolegend, USA; JC1 was purchased from Sigma Chemical Co. (St. Louis, MO). ST03 was synthesized as previously described [30] with a purity of 97.7% (determined by HPLC).

Immunoblotting

ST03 treated and control cells were harvested and lysed in RIPA buffer supplemented with Protease Inhibitor Cocktail (Sigma). Protein concentration was determined by the Bradford method, and 40 μg of protein were resolved by SDS-PAGE followed by transfer onto PVDF membrane. The appropriate protein bands were cut and antibody hybridization performed by standard immunoblotting procedures. The protein bands were detected using the enhanced chemiluminescence substrate (Biorad) and images acquired on the Biorad XR+ Gel doc system. Protein band quantification was performed using GelQuant.Net, BiochemLab solutions

Cell cycle analysis

Cell cycle analysis was performed by flow cytometry with PI stained cells. Both PA1 and A2780 cells were seeded onto 6 well plate at a density of 1×10^5 cells/well. Next day the cells were treated with ST03 (10, 50, and 75 nM) for 48 h. Post incubation cells were harvested, washed in ice-cold 1X PBS and incubated in citrate buffer (0.1% trisodium citrate, 0.03% NP-40, 100 μg/ml RNase A) for 37 °C for 15 min. PI (4 μg/ml) was added and incubated for 5 min at RT. 10,000 events were acquired by flow cytometry (Gallios, Beckman Coulter) and histogram represented using the in- built Gallios software (version 1.2, https://www.mybeckman.in/)

JC-1 mitochondrial membrane potential (ΔΨm) assay

The Mitochondrial staining kit (Sigma CS0390) was used to perform this assay. Briefly, PA1 and A2780 cells treated with ST03 for 48 h were harvested and resuspended in staining buffer containing JC-1 and incubated in the dark for 20 min at 37 °C with 5% CO2. Valinomycin was used as a positive control. Post incubation cells were resuspended in fresh buffer and fluorescence of the JC1 with 10,000 events was acquired by flow cytometry (Gallios, Beckman Coulter).

Examination of intracellular ROS accumulation

Intracellular ROS levels were examined by staining the cells with H2DCFDA (2′,7′-dichlorodihydrofluorescein diacetate) by flow cytometry. Both PA1 and A2780 cells were cultured in 35 mm culture dish at a density of 1 × 105 cells and treated with 50 nM ST03 for different time points (10, 20 and 30 min). The cells were harvested post different time points, washed in PBS, stained with H2DCFDA for 30 min and analyzed by flow cytometry (Gallios, Beckman Coulter). H2O2 treated cells served as a positive control in this experiment. ROS production was measured by examining the degree of shift in the histogram by considering Median Fluorescence Intensity as a parameter.

For spectrometric ROS measurement, PA1 cells and A2780 cells were plated at 20,000 cells/well on opaque 96 well plate. Post 24 h, the cells were washed in 1X PBS and incubated with H2DCFDA (10 μM) with different concentrations of ST03 also in combination with 20 mM N-acetylcysteine (NAC) in 1X PBS for 1 h. Post incubation, the fluorescence was measured at ex 485/em 535 using a fluorescent microplate reader. 200 μM H2O2 was used as a positive control for this experiment.

Real time PCR

Total RNA was extracted from both A2780 and PA1 cells treated with different concentrations of ST03 using manufacturers protocol (RNAisoPlus, Takara). 2 μg RNA was used for cDNA synthesis (PrimeScript RT Reagent Kit, Takara). qPCR was performed in triplicates and assays performed using the StepOnePlus Real-Time PCR System (Applied Biosystems). The primer sequence used were ND2 F- CACA-GAAGCTGCCATCAAGTA, ND2 R-CCGGAGAGTATATTGTTGAAGAG, CYTB F- TCATCGACCTCCCCACCCCATC, CYTB R-CGTCTCGAGT-GATGTGGGCGATT, ATPase 6 F-GCCCTAGCCCACTTCTTACC, ATPase 6R-TTAAGGCGACAGCGATTTCT.

Cell viability assay

100,000 cells per well of a 24 well plate was seeded with either A2780 or PA1 cells with ST03 and with NAC and treated for 48 h. Post incubation, cell number for each condition was determined and plotted as bar graphs.

Transwell migration assay

Transwell migration assay was performed using Corning Inc. 24-well insert with 8 μm pore size. Briefly, 1×10^5 PA1 cells treated with different concentrations of ST03 for 48 h were seeded onto each insert in serum free media. The bottom chamber was filled with complete media and incubated for 5 h. Post incubation, the media was removed, and the insert washed in 1X PBS. The cells were then fixed in 70% Ethanol. Cells present in the inner chamber, which are the non-migratory cells, were removed using cotton and were stained with 0.2% Crystal Violet and imaged. Quantification was performed using ImageJ software (version 1.52a, https://imagej.nih.gov/ij/).

In vivo experiments

Animals

Mice were maintained and experiments conducted as per the rules and guidelines of the Institutional Animal Ethical Committee of IBAB and following Indian national law on animal care and use. The animal experiments conducted for this project were approved by the Institutional Ethical Committee of IBAB, Bangalore, India (Ref. IAEC/IBAB/03/10–7_2018) and also follow the ARRIVE guidelines. Female Swiss albino mice at 6–8 weeks old, with an average weight of 19–22 g, were purchased from Liveon Biolabs Pvt. Ltd., Bangalore, India, and quarantined for 2 weeks the experimental room conditions for acclimatization. Animals were maintained in a room with controlled humidity, temperature (23±3 °C), and light cycles (12 h dark/ 12 h light). They were housed in ventilated polypropylene cages and provided a standard

pellet diet (Liveon Biolabs Pvt. Ltd.) and water ad libitum. The standard pellet diet composed of 21% protein, 5% lipids, 4% crude fiber, 8% ash, 1% calcium, 0.6% phosphorus, 3.4% glucose, 2% vitamin, and 55% nitrogen-free extract (carbohydrates).

Passaging and preparation of Ehrlich ascites carcinoma (EAC) cells for tumor induction on the thigh

Passage EAC cells were maintained in animals by injecting a fixed amount of cells taken from donor mice to the intraperitoneal cavity of recipient mice. Every 7th day, this procedure was repeated for maintaining EAC cells in vivo. On the 7th day, cells were withdrawn from the intraperitoneal cavity, diluted in 1X PBS, counted, and re-injected 1×10^6 cells subcutaneously for developing solid tumor.

Evaluation of the antitumor activity of ST03 in mice models

The tumor measurements were done on the 7th day of tumor induction using Vernier calliper and were segregated into different groups where the average tumor size was maintained constant. Two groups of animals were considered per batch, and every group received 5 animals each. The experiment was repeated three times, and a total of $n = 15$ animals per group was used in the study. Group I animals served as tumor control without any treatment; group II animals received ST03 10 mg/kg b.wt (bodyweight) as an intraperitoneal injection, every alternative day throughout the study. The dose was selected based on the preliminary studies. The animal weight was recorded, and tumor size was measured every alternative day using a Vernier calliper. The volume was calculated by the formula: $V = (ab^2)/2$, in which "a" and "b" are major and minor diameters respectively. At the end of the experiment period, animals were sacrificed, organs, including the tumor, collected for histological staining and protein extraction.

Chemo preventive effect of ST03

The preventive chemo effect of ST03 was examined by taking two different groups ($n = 5/group$). Group 1 received 15 doses of pre-treatment with ST03 (alternate days) before tumor injection and continued with 15 more doses of post tumor injection. Group 2 was considered as tumor controls and did not receive ST03 treatment. The tumor volume was measured from the 7th day of tumor injection. The experiment was repeated two independent times, and the tumor volumes, body weight, and other physiological parameters were measured and compared with control animals.

Histological evaluation of tumor and organs

Hematoxylin and Eosin staining

The fixed tissues were processed as per the standard protocols [69], and paraffin blocks were prepared. 10 μm sections were taken using a rotary microtome (Leica Biosystems, Wetzlar, Germany) and stained with Hematoxylin and Eosin as per standard protocols [24]. Stained sections were observed under a microscope and images captured.

Immunohistochemistry and immunoblotting

IHC analysis of the formalin-fixed treated tumor and control tumor were performed as per standard protocols [25]. Briefly, 5 μm sections were taken using the rotary microtome (Leica Biosystems, Germany). The slides were deparaffinized, rehydrated, and treated with 3% H_2O_2 in 1X PBS. Antigen retrieval was carried out by boiling the slides in 10 mM sodium citrate buffer, pH 6. The sections were incubated with blocking reagent (5% goat serum (Sigma)/ 1% BSA) for 30 mins, followed by mouse anti-PCNA antibody (1:100) for 1 h RT or O/N at 4 °C, 1 h in biotinylated Anti-mouse IgG (1:200), and 15–20 min in Streptavidin-HRP (1:1000) for the signal amplification. The color was developed using DAB- H_2O_2. The slides were then mounted with DPX, and images captured using a light microscope. For immunoblotting studies, the tumor tissue was crushed in liquid nitrogen and proteins extracted in RIPA buffer. Protein concentration was estimated by the Bradford method, and 40 μg protein was used for SDS-PAGE.

Evaluation of ST03 toxicity in experimental animals

The toxicity induced by ST03 compound was analyzed during the treatment period by measuring and comparing the body weight of treated animals with the tumor controls and were plotted with error bars. At the end of the study, blood samples were collected to study the treatment effect on physiological functions. Blood samples were collected in heparinized tubes for RBC, WBC cell count. Also, blood without heparin was collected, and serum was separated for liver and kidney function tests such as Alanine aminotransferase (ALT), Aspartate aminotransferase (AST), and urease test using AUTOSPAN Liquid Gold ALT, AST, Urease kit.

ST03 bioavailability studies

Chromatographic conditions

The analytes' separation and retention were performed on a Shiseido cap cell pack C18 column (S-5, 4.6 mm × 250 mm). 2% Acetic acid in HPLC grade water (A) and HPLC grade Acetonitrile (B) (40:60, v/v) was used as a mobile phase for ST03 and only acentonitrile was used for curcumin. The flow rate was 1 mL/min, the detection wavelength was 312 nm for ST03 and 369 nm for curcumin, column temperature was room temperature, and 20 μL of samples were injected. The mobile phase was filtered through a 0.45 μm membrane filter and degassed before use.

Sample preparation

Swiss albino mice were divided into four groups ($n = 2$). Each group was administered ST03 orally, ST03 intraperitoneally, curcumin orally or curcumin intraperitoneally. The mice in each group was administered a single dose of ST03 at 10 mg/Kg b.wt or curcumin at 20 mg/Kg b.wt and blood collected at different time points (5, 10 and 15 min and 1, 3, 6, 12 and 24 h). Plasma samples were collected by centrifuging at 1500 rpm for 15 min. Extraction of analyte from plasma was done using protein precipitation procedure, an equal volume of acetonitrile was added to the plasma, and vortexed for 2 min, followed by centrifugation at 14,000 rpm 5 min and the upper organic layer was collected and used for the analysis.

HPLC analysis

To evaluate linearity, mice plasma calibration curve was prepared with a gradient of ST03 (97.7% purity) (1, 10, 50 and 100 μM) and curcumin solution (1, 5, 10, 50 and 100 μM, in mobile phase). Selectivity was assessed by comparing the chromatograms of blank plasma and plasma spiked with known concentrations of ST03. LOQ and LOD for both ST03 and curcumin were calculated using linear regression method. Statistical analysis: For each experiment, the ANOVA test was carried out based on the number of groups using the Graph pad prism7 tool, and the treatment results were compared with the control sample to find out the statistical significance. P values less than 0.05 were considered significant, and the bar graphs are represented as Mean +SEM.

Results

ST03 induced cell death without affecting the cell cycle

Cell cycle analysis was performed using ovarian cancer cell lines, PA1 (teratocarcinoma), and A2780 (epithelial) treated with different concentrations of ST03 (10, 50, and 75 nM) for 48 h and subjected to flow cytometry after staining with Propidium Iodide. The results showed an accumulation of cells at the Sub G0/G1 stage after 48 h of treatment (Fig. 1). At 50 nM concentration, ∼ 70% of PA1 cells accumulated at the sub G0/G1 stage (Fig. 1A), whereas ∼ 60% in A2780 cells (Fig. 1B). However, there was no notable cell cycle arrest observed at 48 h of ST03
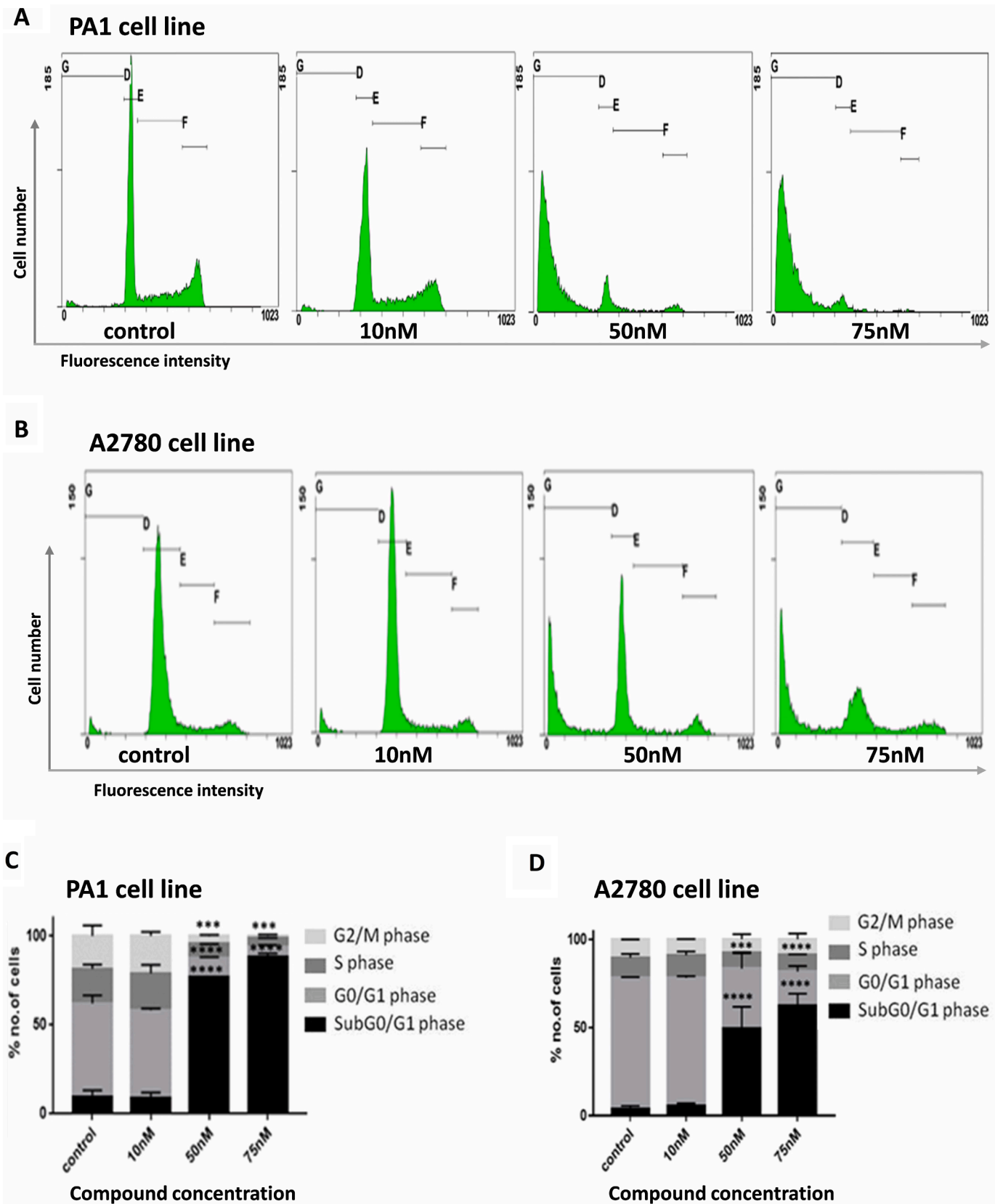
Fig. 1. Effect of ST03 on cell cycle distribution in ovarian cancer cell lines: Cell cycle distribution of PA1 and A2780 cells treated with different concentrations of ST03 (10, 50, and 75 nM) for 48 h were analyzed by flow cytometer. The horizontal lines in the graph denotes cell populations in each phase of the cell cycle (G-D denotes cells in G2/M phase, D and E in S phase, E-F in G0/G1 phase and after F in sub G0/G1 phase). Bar diagram shows percentage of cells distributed in each phase of cell cycle. Each experiment was repeated for a minimum of 3 times and plotted as bar graphs with error bars. The p value was calculated between control and ST03 treated groups, where, *: p value < 0.05, **: p value <0.005, ***: p value < 0.0001, ****: p value < 0.00001.

treatment in both the cell lines.

ST03 alters mitochondrial membrane potential (Δψm) and induces intrinsic pathway of apoptosis

The mechanism of ST03 induced cytotoxicity was studied by treating ovarian cancer cell lines PA1 and A2780 with increasing concentrations of drug for 48 h and stained with JC1. JC1, a cationic dye, accumulates in the mitochondria, forming aggregates, exhibiting red fluorescence in healthy cells. In apoptotic cells, the mitochondrial membrane is leaky, JC1 cannot form aggregates and exhibits green fluorescence [49,55]. The flow cytometry analysis (Fig. 2A,B) showed an increase in the green population upon ST03 treatment in both the cell lines, indicating mitochondrial damage. No damage to mitochondria was observed in vehicle control.

Loss of mitochondrial membrane potential is a distinctive feature of
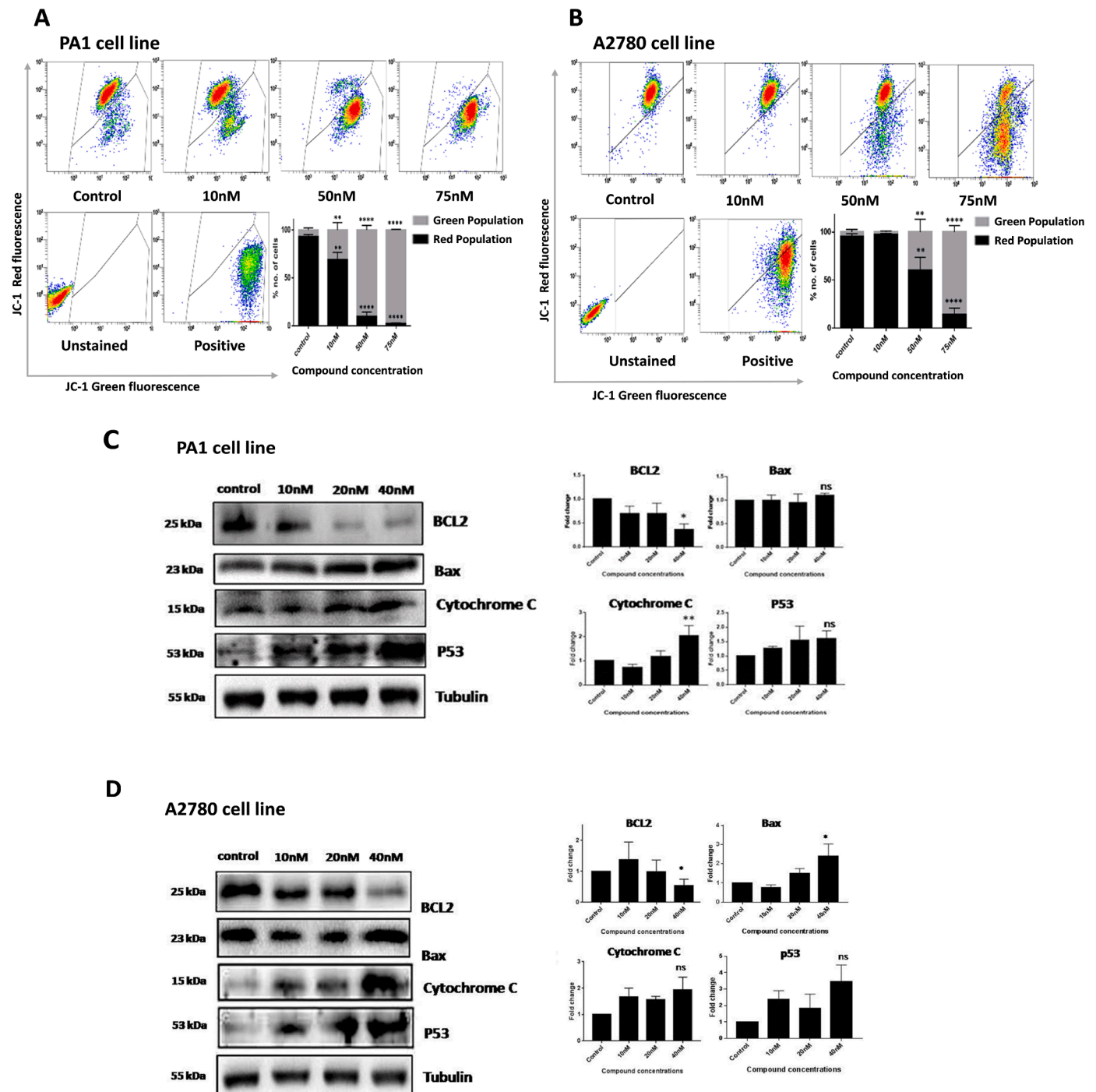
Fig. 2. Examination of mitochondrial depolarization and expression of mitochondria related proteins in ovarian cancer cell lines upon ST03 treatment: 2 A, B depicts the effect of ST03 treatment on mitochondrial membrane potential examined by JC1 staining in PA1 cells (a) and A2780 (b). Spectral shift from red to green as a result of ST03 treatment (10, 50, and 75 nM) is shown in dot plots and the percentage was plotted as bar graph. Valinomycin was used as positive control. Median fluorescent intensity (MFI) was plotted as bar graph. C represents the mitochondrial protein expressions upon ST03 in PA1 cells and D represents the mitochondrial protein expressions upon ST03 in A2780. Each experiment was repeated for a minimum of 3 times and the p value was calculated between control and ST03 treated groups, where, *: p value < 0.05, **: p value <0.005, ***: p value < 0.0001, ****: p value < 0.00001.

apoptosis. The expression of outer mitochondrial membrane proteins Bcl2 (antiapoptotic), and Bax (proapoptotic) was assessed using western blotting. In both cell lines, a significant decrease in Bcl2 expression and an increase in Bax expression was observed upon treatment with 40 nM ST03 (Fig. 2C, D). Cytochrome C release from inner mitochondrial membrane space initiates the process of apoptosis [20] . An increase in Cytochrome C was observed with increasing concentrations of ST03 treatment in both PA1 and A2780 cells (Fig. 2C, D). Proapoptotic p53 also showed upregulation upon ST03 treatment. In our previous study, we reported a caspase-mediated intrinsic apoptotic pathway in ovarian
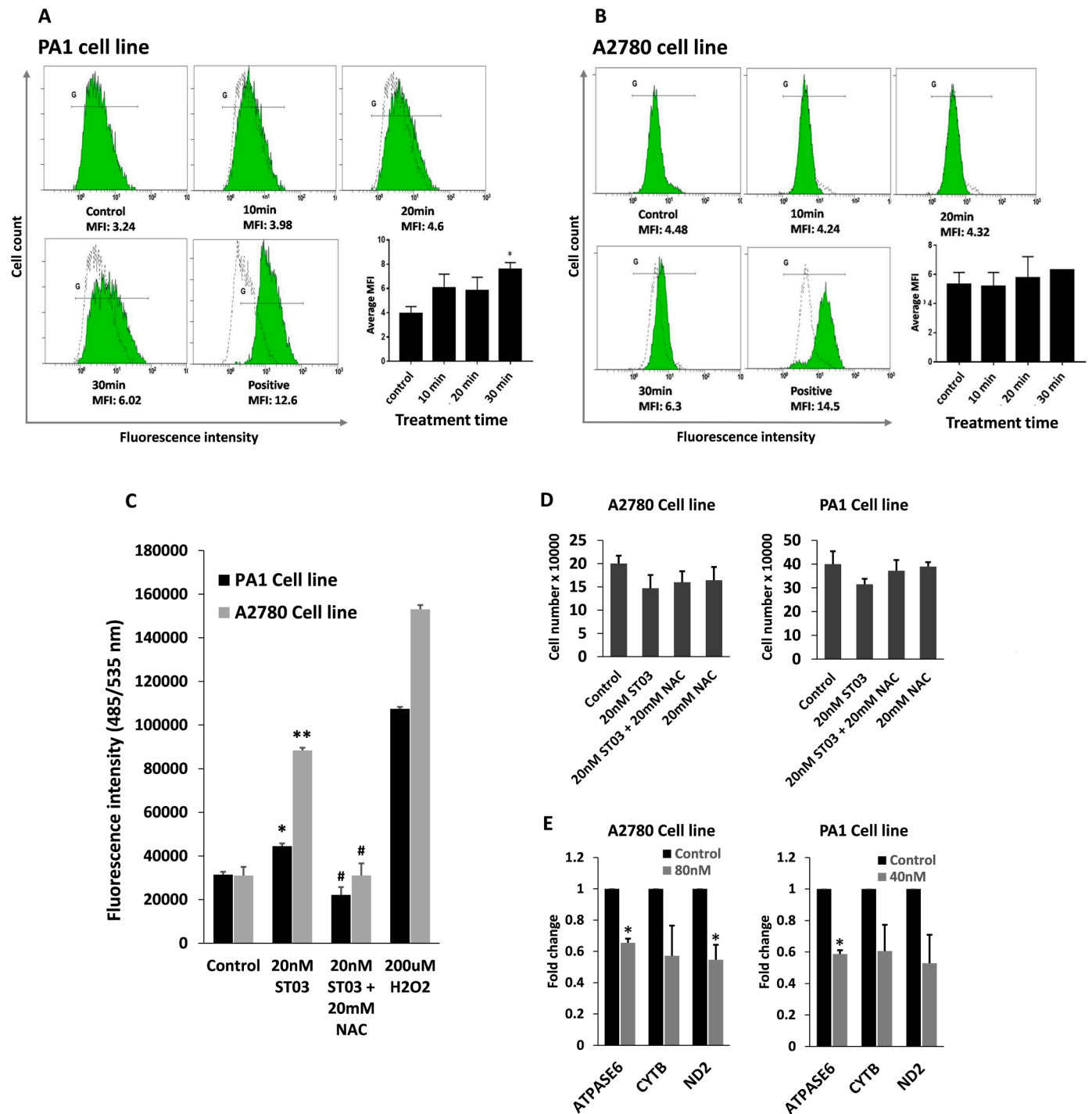
Fig. 3. ROS induction upon ST03 treatment in ovarian cancer cell lines, its suppression by NAC and its effect on OXPHOS genes: 3 A,B represents the ROS assay histograms. PA1 and A2780 cells treated with ST03 for different time points were stained with H_2DCFDA and subjected to flow cytometry analysis. A shift in the histogram when compared to control histogram (dotted lines) shows presence of ROS due to ST03 treatment. Median fluorescent intensity (MFI) was plotted as bar graph. C Graph represents the ST03-induced ROS in A2780 and PA1 cells. Graph was plotted against the fluorescence intensity measured by H_2DCFDA staining. 20 mM N-acetyl cysteine (NAC) was used as ROS scavenger. Treatment with H_2O_2 served as the positive control.. D represents the cell proliferation upon 20 nM ST03 and with 20 mM NAC for 48 h. E Represents transcript levels of mitochondrial oxidative phosphorylation genes upon treatment with ST03 after 48 h of treatment. Each experiment was repeated for a minimum of 3 times and the p value was calculated between control and ST03 treated groups, where, *: p value < 0.05,. # represents significancy between the ST03 treated and ST03 with NAC where p value < 0.0001.

cancer cell line treated with ST03 [30] . Together, these findings confirm that ST03 activates a mitochondrial-mediated intrinsic apoptotic pathway in ovarian cancer cell lines.

ST03 treatment leads to peak ROS levels within 1 h and reduces mitochondrial OXPHOS gene expression in 48 h

One of the mechanisms by which drugs induce mitochondrial damage is the generation of ROS [64]. To investigate the effect of ST03 on ROS production in the ovarian cancer cell lines, we utilized the fluorogenic dye H_2DCFDA ($2',7'$–dichlorofluorescein diacetate). The cells were treated with ST03 for 10, 20, and 30 min, stained with H_2DCFDA, and the fluorescence detected via flow cytometry. Compared to vehicle control, the shift in the fluorescence histogram (measured by Median Fluorescence Intensity) was considered a measure of intracellular ROS. In PA1 cells, at 50 nM, ST03 treatment-induced ROS production within 10 min and gradually increased with time (Fig. 3A). Whereas, A2780 showed a shift in the histogram at 30 min with 75 nM ST03 concentration (Fig. 3B). Cells treated with H2O2 were used as the positive control. These results indicate that ST03 treatment triggers ROS production stimulating oxidative stress as an initial response, which then initiates the cascades of cell death programs in these ovarian cancer cell lines. Further to establish ST03 induced mitochondrial ROS is an early event initiating the change in mitochondrial membrane permeability and subsequent changes in the mitochondrial OXPHOS transcription, both PA1 and A2780 cells were treated with 20 nM and 40 nM for various time points 15 and 30 min, and 1, 2, 24 and 48 h. Both cell lines attained peak ROS levels after 1 h of 20 mM ST03 treatment. Further, addition of 20 mM NAC, a ROS scavenger blocked ST03 induced increase in ROS (Fig. 3C) in both cell lines. In accordance with diminished levels of ROS, decrease in cell death was evident after 24 h treatment in presence of NAC (Fig. 3D). This indicated that ST03 induced ROS production is an early event driving the changes in mitochondrial membrane and regulating cell death. After 48 h of treatment, a decrease in the transcription of mitochondrially encoded OXPHOS genes (ND2 from complex I, CYB from Complex III and Atpase6 from Complex V of the ETC) was observed in both cell lines (Fig. 3E) indicating that ST03 alters ROS production by directly interfering with mitochondrial OXPHOS gene transcription. ST03 showed ROS induction, followed by mitochondrial damage and cell death by a mitochondrial pathway in vitro in both ovarian cancer cell lines.

ST03 inhibits the migration of ovarian cancer cells by altering MMP1

Transwell migration assay examined the migratory capacity of the ovarian cancer cell line PA1 treated with ST03. A dose-dependent decrease was observed in the migratory pattern of PA1 cells at 40 nM ST03 treatment showing a 60% reduction in migration (Figs. 4A, 5B). Since migration involves extracellular matrix degradation, we evaluated the expression of MMP1, a crucial protease involved in this process, and observed a significant decrease in its expression at 40 nM (Fig. 4C, 4D).

ST03 treatment reduced tumor growth in mice

To test the impact of ST03 in-vivo, mouse syngeneic breast adenocarcinoma model was used. To begin we tested the effect of drug on human breast cancer cell lines hormone negative (MDA-MB-231, and MDA-MB-468) and positive cells (MCF7). ST03 induced cytotoxicity in all the breast cancer cell lines at IC50 ranging from 166 to 301 nM (Supplementary Fig. 1). The hormone positive MCF7 had the least IC50. EAC is a spontaneous breast cancer mice model and is widely used for testing anti-cancer drugs.

EAC induced Swiss albino mice model was used for studying the in vivo activity of ST03. Based on pilot studies, we found that 10 mg/kg b.
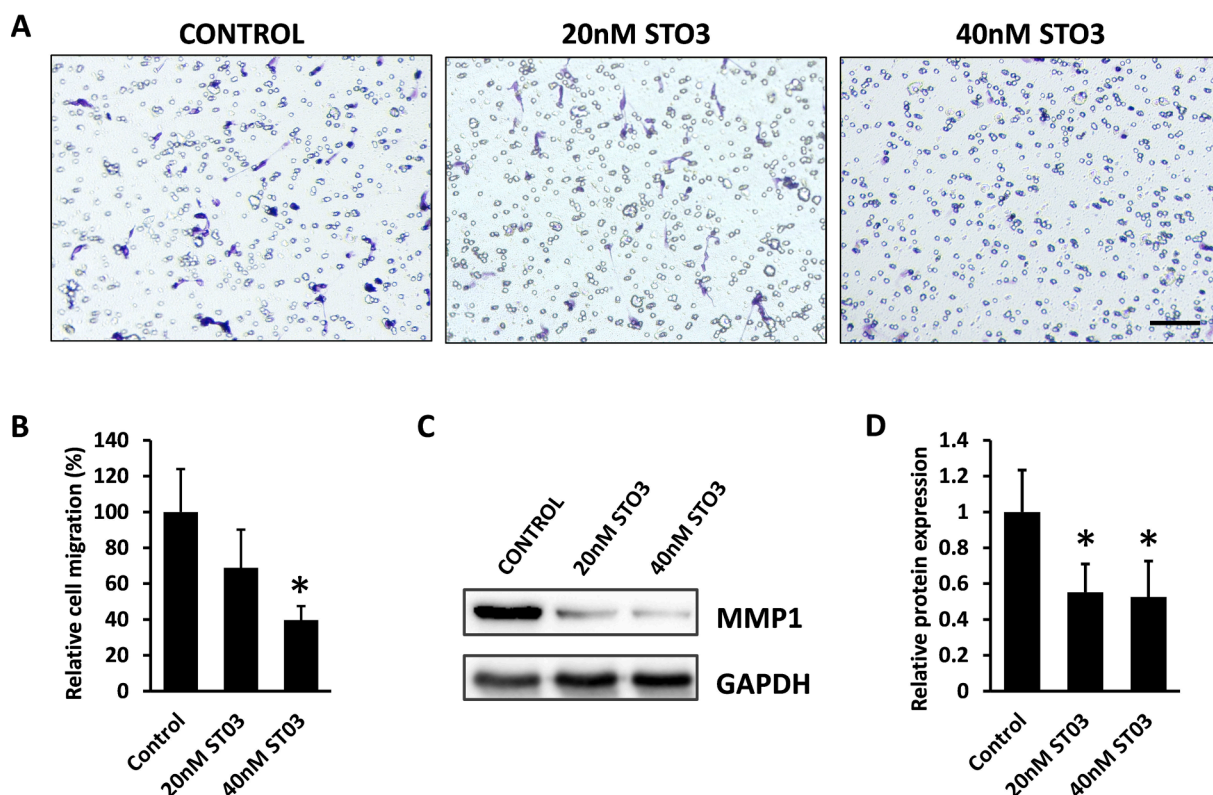
Fig. 4. Effect of ST03 on migration and expression of MMP1 in PA1 cells. A: represents the migration of PA1 cells upon ST03 treatment performed by transwell migration assay. The scale bar represents 150 μm. B: represents the migration quantification C: represents the protein expression of MMP1 in PA1 cells upon ST03 treatment where the membrane corresponding to the protein band were cut and hybridized with the antibody D: represents the MMP1 protein quantification. Each experiment was performed minimum 3 times and P value < 0.05 is represented as significant.
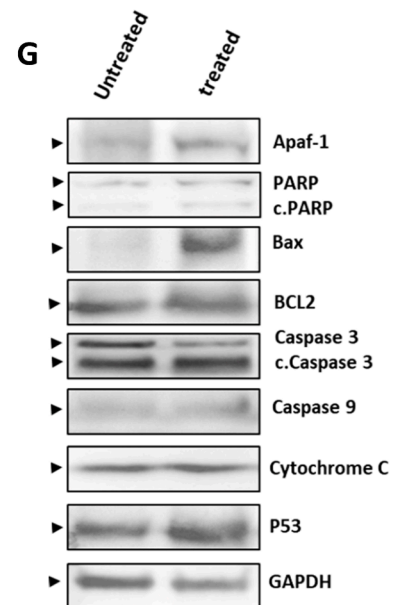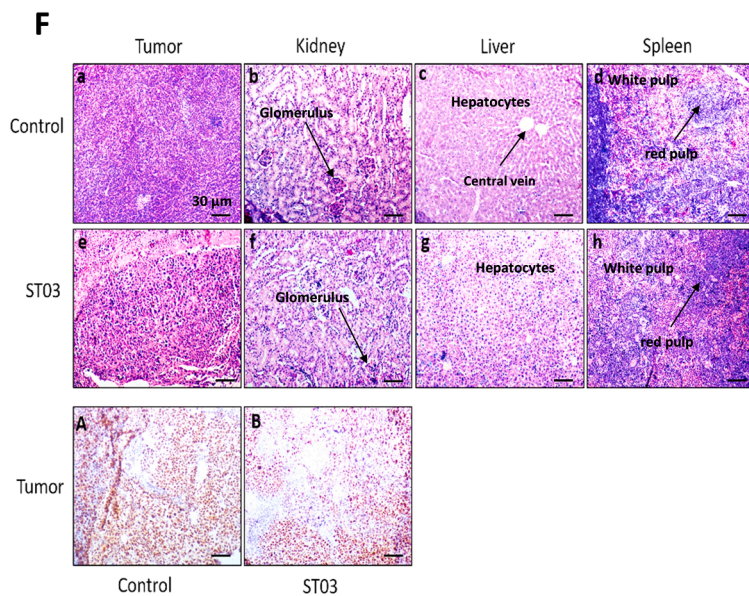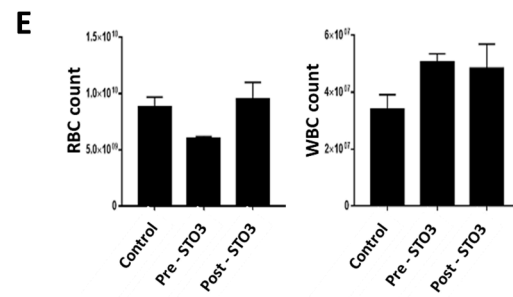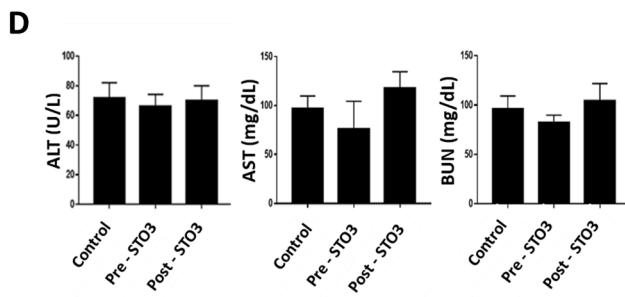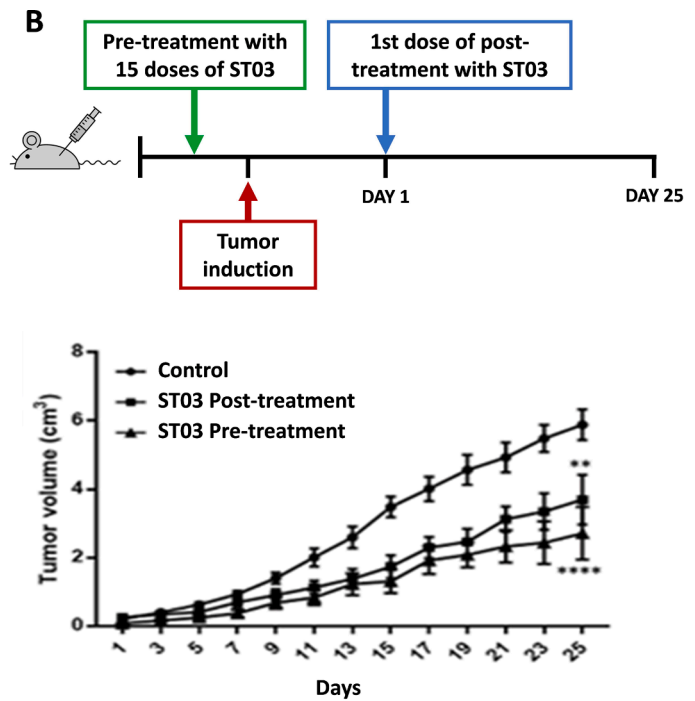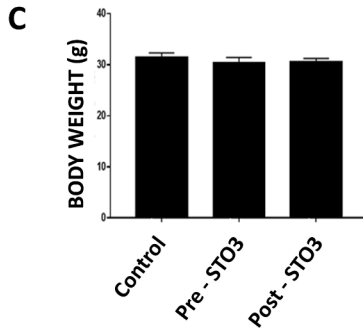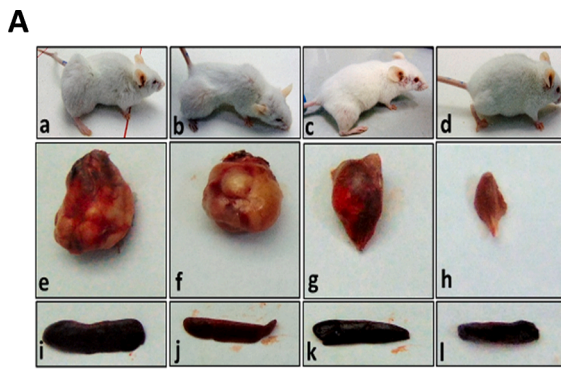
(caption on next page)

Fig. 5. Evaluation of effect of ST03 on in vivo tumor growth: EAC cells (1×10^6 cells/ animal) were injected to induce solid tumors. After the 7th day of injection, i.p injection with ST03 (10 mg/ kg b.wt) was started every alternate day throughout the experiment period. For pre-treatment experiment, animals were pre-treated with 15 doses of ST03 (10 mg/ kg b.wt) and then tumor was induced. A The gross appearance of a. control, b. ST03 post treatment, c. ST03 pre-treatment, d. normal mice e. control tumor, f. ST03 post treatment tumor, g. ST03 pre-treatment tumor, h. normal thigh, i. Control spleen, j. ST03 post treatment spleen, k. ST03 pre-treatment spleen, l. normal spleen. B represents tumor volume after ST03 pre and post treatments C represents body weight of animals at the end of the study D Represents Blood ALT, AST, Urease test results plotted as bar graph. Blood was collected at the end of the study E Represents RBC and WBC counts of experimental animals plotted as bar graph F Represents Histopathological analysis of tumor and organs after ST03 treatment. At the end of the study, tumor tissue and organs were collected and used for histological analysis. Representative images of H&E stained sections of a. control tumor, e. ST03 post-treatment tumor b. control kidney, f. post-treatment kidney, c. control liver, g. ST03 post-treatment liver d. control spleen, h. ST03 post-treatment spleen, A. PCNA stained paraffin sections of control tumor, B. ST03 post-treatment tumor. G Western blot analysis of tumor tissues of untreated control and ST03 post-treatment animals. Scale bar represents 30 μm.

wt. exhibited tumor growth reduction without noticeable side effects (data not shown). After the 7th day of the inoculation of EAC cells, mice bearing tumors were treated with ST03 every alternate day throughout the experiment (25 days). The results showed a significant reduction in tumor growth in ST03 treated mice compared to untreated control mice bearing tumor (Fig. 5A, 5B). The tumor tissue's gross appearance after the 25 days of treatment showed a significant difference in tumor size (Fig. 5A) compared to the control tumor. The chemopreventive effect of ST03 was also studied by pre-treating animals with 15 alternate doses of ST03 (10 mg/kg b. wt.), no treatment was given during tumor inoculation followed with post-treatment as described above after tumor induction. The results showed a significant reduction in tumor growth in pre-treated animals when compared to controls (Fig. 5A, 5B).

Similarly, tumor growth suppression was significant in pre-treated animals than in post-treated animals. Enlargement of spleen is associated with tumor growth. One of the indications of a reduction in tumor size is the restoration of the spleen to its standard size. ST03 induced reduction in tumor growth was associated with a reduction in spleen size compared to the enlarged spleen in untreated animals. These results show that ST03 can act both as a chemo preventive and chemotherapeutic agent in anticancer therapy.

ST03 treatment reduces tumor growth by activating apoptotic pathway

Western blot and immunohistochemistry analysis were carried out to understand the cell death mechanism *in vivo*. A significant reduction of tumor cells in the ST03 treated samples compared to control tissue was observed using Hematoxylin and eosin staining (Fig. 5F). Also, a high level of PCNA staining was observed in the control tumor vs. treated, confirming the observation of a reduction in proliferating cells in treated tissue (Fig. 5F (A)(B)).

Further, western blotting of the extracts from the treated tumor showed significant up-regulation of proapoptotic proteins (Fig. 5G). Proteins such as Bax, p53, Apaf-1, caspase 9, cleaved PARP, cleaved caspase 3, and cytochrome C were upregulated. Unlike in in-vitro experiments, where antiapoptotic protein Bcl2 was down-regulated, there was an up-regulation observed in vivo. These results suggest that tumor reduction by ST03 was brought about by tilting the balance between proapoptotic vs. antiapoptotic signals and activation of mitochondrial-mediated cell death pathway.

Toxicity studies on ST03 treated mice

The toxicity induced by ST03 treatment was examined by recording the body weight throughout the experiment time frame. There was no notable weight reduction observed in pre- and post-treatment animals (Fig. 5C). We performed hematological, liver, kidney functional assays to study the side effects of ST03. Interestingly, an increase in the number of WBCs in the ST03 treated groups compared to the control group was observed (Fig. 5E), which might correlate with the immune activation property of the ST03 compound. No significant change was observed in the number of RBCs (Fig. 5E). No significant change in ALT, AST, and urea levels were observed (Fig. 5D), suggesting no apparent liver or kidney toxicity. H&E of tumor tissues from the control group demonstrated a large number of highly stained and densely packed nuclei

(Fig. 5F (a)), indicative of proliferating cells compared to the treated group (Fig. 5F (e)). Also, in the tumor tissues of treated group cells with fragmented nuclei were observed, indicating apoptosis. To test for any histopathological changes upon treatment with ST03, sections of the kidney (Fig. 5F (b, f)), liver (Fig. 5F (c, g)), and spleen (Fig. 5F (d, h)) tissues were taken and H&E staining was performed. The liver sections of ST03 treated group showed normal architecture of hepatocytes and kidney of the ST03 treated group showed normal glomeruli structure. Overall, the sections did not show any significant cellular morphology and integrity changes on treatment with ST03, which indicates no pathological changes. Hence our study shows that ST03 did not exert any major systemic changes.

ST03 showed better bioavailability than curcumin

Bioavailability of the ST03 and curcumin was performed using the plasma of a single dose 10 mg/kg body weight ST03 and 20 mg/kg body weight curcumin treated female Swiss albino mice. Two different modes of drug administration were used. The drug was administered orally and intraperitoneally. The plasma collected at different time points (5, 10 and 15 min and 1, 3, 6, 12 and 24 h) was analyzed using the Shimadzu LC-20A system equipped with the UV–visible spectrometry detector SPD-M20A photodiode array. The lowest amount of ST03 detectable was 1.65 μM and limit of quantitation was 5 μM. The maximum concentration of ST03 when administered orally was 55.2 μM at 2 h (Fig. 6A). In contrast the maximum concentration ST03 was 98.4 μM at 8 h intraperitoneally (Fig. 6C). The drug t1/2 for oral was 3 h. Curcumin on the other hand, was 13.7 μM at 15 min and intraperitoneally was 2.7 μM at 3 h (Fig. 6B. 6D). Curcumin was bioavailable for longer duration when given intraperitoneally.

Discussion

Cancer is the second most deadly disease and a major public health concern worldwide [53]. One of the biggest challenges is to develop an anticancer drug with low toxicity and side effects. Curcumin has widely attracted scientific attention from its discovery by Vogel and Pelletier [59] as a novel anticancer agent due to its multifunctional characteristics such as anti-oxidant, anti-inflammatory, and antitumor properties [41]. Curcumin has shown anticancer properties on various cancer types such as colorectal cancer, pancreatic cancer, lung cancer, breast cancer, head and neck cancer, prostate cancer, and brain cancer [5]. However, there has been limited clinical use of curcumin due to its low stability and bioavailability in the in vivo system [48]. Several modifications of curcumin have been made to enhance its potency and stability. The presence of α, β unsaturated ketones, is responsible for the multitargeted effect of curcumin, and is also responsible for its low stability [13,22]. Modifications of curcumin, which have hydrogen bond acceptors such as oxygen, nitrogen, chlorine atoms, have shown enhanced potency and ability to revert multi-drug resistance (MDR) [12,33]. Previous reports have shown that the curcumin derivative 1,2-bis[(3E,5E)−3,5-dibenzylidene-4-oxo-1-piperidyl]ethane-1,2-dione induce cytotoxicity in multiple cancer cell lines in vitro with greater potency than the parent compound curcumin [50]. Here the presence of oxygen atoms, amidic groups, and aryl rings present in its structure improved its potency. The
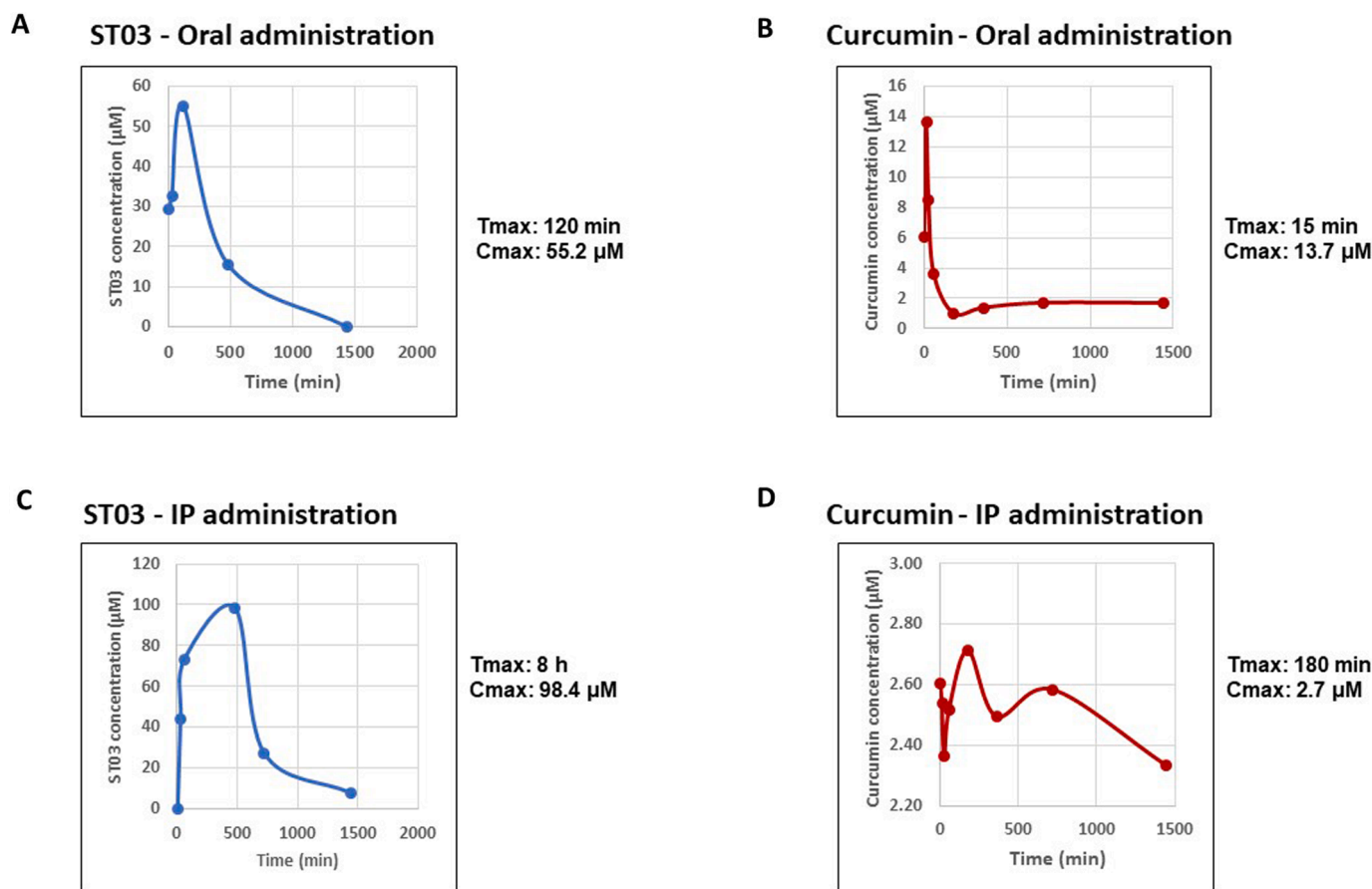
Fig. 6. Pharmacokinetic profile of ST03 compared to curcumin. Plasma concentration-time profiles of oral and intraperitoneal administration of ST03 and curcumin was determined by HPLC-UV. ST03 (10 mg/kg bodyweight) and curcumin (20 mg/kg bodyweight) was administered both orally and intraperitoneally into Swiss albino mice. Plasma concentrations are represented in each graph along Cmax and Tmax of the drug. A, B represents plasma concentrations of ST03 on oral and IP administration respectively. C, D represents plasma concentrations of curcumin on oral and IP administration respectively. Each point represents the mean concentration ($n = 2$).

addition of four chlorine atoms to the structure improvised the potency of ST03 compound (1,2-bis[(3E,5E)−3,5-bis[(2-chlorophenyl)methyl-ene]−4-oxo-1-piperidyl]ethane-1,2-dione) [30], which is 5–6 fold better than the 1,2-bis[(3E,5E)−3,5-dibenzylidene-4-oxo-1-piperidyl] ethane-1,2-dione reported and ~100 fold better than the parent compound curcumin.

In the current study, we elucidated the cell death mechanisms induced by ST03 in ovarian cancer cell lines PA1 and A2780 in vitro and its anticancer activity in vivo in EAC tumor-bearing mice models. Our previous study has documented that ST03 selectively induces toxicity in cancer cells compared to normal cells [30]. Interestingly, ST03 showed better cytotoxicity on PA-1 cells, an undifferentiated teratocarcinoma with stem cell-like property than on epithelial cell A2780. A similar effect of curcumin has been observed in the context of breast cancer cell line where curcumin showed a better effect on mesenchymal MDA-MB-231 than epithelial MCF7 [28]. ST03 exhibited 100 fold better cytotoxicity on both ovarian cancer cells as compared to curcumin. Also, ST03 blocked the migration of PA1 cells, accompanied by the downregulation of MMP1, a crucial protease involved in ECM degradation [29]. Curcumin regulates ECM degradation in several cancer cell lines by modulating MMP activity [11,45]. One of the major challenges in controlling cancer is metastasis. Therefore, drugs which can modulate MMP activity can be used to target metastasis. In this regard, curcumin derivatives have been designed using QSAR methods to target MMP activity [31]. ST03 seems to be a promising candidate exhibiting its inhibitory on migration and invasion via downregulation of MMP1 in the ovarian cancer cell line.

There are several pathways by which drugs can induce cell death. ST03 induced cell death via the intrinsic pathway of apoptosis in both ovarian cancer cell lines as evidenced by depolarization of mitochondrial membrane potential and upregulation of pro-apoptotic proteins like Bax, cytochrome-c, and downregulation of antiapoptotic protein like Bcl2. Curcumin is known to induce apoptosis in tumor cells by disrupting the mitochondrial membrane potential and activating a cascade of caspase pathways [47,57]. In A2780 curcumin induced cell death by activating caspases [67]. ST03 induced alteration in the ratio of BCL2-Bax was observed in both cell lines after treatment. It is known that Bax oligomerizes with Bak, creates pores on the mitochondrial membrane, leading to leakage of proteins such as cytochrome C [9]. ST03 treatment led to change in the antiapoptotic/ apoptotic ratio and change in MMP leading to cell death.

ST03 induced ROS production, similar to its parent curcumin [6,7, 56], Mitochondria is the main source for ROS production in the cell. Many chemotherapeutic drugs alter ROS production to induce cell death [63]. ST03 induced ROS production in both ovarian cancer cell lines PA-1 (40 nM, 10 mins) and A2780 (75 nM, 30 mins). Interestingly, at 20 nM both cell lines attained peak ROS after1 h of treatment. It is known that ROS levels change over time and a critical level would decide cell death vs cell survival [62]. N-acetyl cysteine (NAC), a ROS scavenger abrogated cell death induced by ROS further emphasizing the role of ST03 induced mitochondrial ROS in cell death. Elevated cellular ROS production can be attributed to mitochondrial ETC or inhibition of the cellular antioxidant system. The ROS production happens during oxidative phosphorylation in mitochondria. ST03 induced changes in

mitochondrially encoded OXPHOS genes (ATPASE6, ND2 and CYTB) to alter ROS production. Also, metformin, tamoxifen, α-tocopheryl succinate (α-TOS), and 3-bromopyruvate (3BP) have been shown to inhibit ETC disrupting the function of respiratory complexes and inducing high levels of ROS leading to cancer cell death [21]. ST03 induced cell death by targeting mitochondria; destabilizing membrane and altering genes involved in oxidative phosphorylation.

Based on the exciting in vitro results, in vivo activity of ST03 on EAC induced tumor-bearing mice models was conducted. The mouse breast adenocarcinoma cell line, EAC (Ehrlich ascitic carcinoma), has been established for testing anticancer compounds in vivo [37]. EAC grows in all strains of mice models aggressively, which induces local inflammatory responses and creates favorable conditions for tumor growth. ST03 dosages of 10 mg/kg (15 doses) were sufficient to inhibit tumor growth in the tumor allograft tested without adverse systemic toxicity. Whereas curcumin is reported to exhibit its antitumor activity in vivo at 800 mg/kg of body weight and with encapsulated dendrosome, the effective dosage is reduced to 40 mg/kg of body weight [19]. In xenograft models, curcumin has been reported to be effective at a twice-daily dosage of 50 mg/kg b.wt in nude mice [18,35]. ST03 also led to no apparent organ toxicity as the ALT, AST, and urea levels were near normal. Also, hematological parameters such as RBC and WBC count were close to normal, indicating no systemic toxicity by ST03. It is important to note that chemotherapeutic drugs have side effects such as anemia and myelosuppression [36]. Interestingly an increase in WBC was observed after ST03 treatment, as observed in immunomodulators like levamisole [8,43]. Immunomodulation by ST03 is under investigation.

The effectiveness of ST03 observed in mouse models of tumour can be attributed to its enhanced bioavailability compared to its parent compound curcumin. The bioavailability of ST03 was ~14 folds more than curcumin orally. The cmax was at 2 h for oral vs 8 h intraperitoneal for ST03 indicating delayed release on i.p. The route of drug administration had an impact on bioavailability in terms of release time and concentration of ST03 and the same was observed for curcumin r. The presence of ST03 in plasma until >12 h both oral and intraperitoneal treatment indicates its enhanced stability compared to curcumin. Further studies will establish the ST03 bioavailability based on various formulations which might increase the stability and bioavailability of the drug. ST03 was completely soluble in 0.6 N HCl. Further, modifications in the drug administration process and methods are being developed to test if the drug's bioavailability can be further increased.

Additionally, ST03 induced minimal organ toxicity and side effects, which might be due to the lower dosage. H & E and PCNA staining showed densely stained and packed nuclei in the untreated control tissue section compared to the treated tissue section indicating the elimination of proliferating cells by ST03. Interestingly, intrinsic apoptotic pathway markers like Apaf-1, Bax, and cleaved caspase 3, cleaved PARP, were upregulated in treated tumor samples compared to untreated control tumor tissue.

Curcumin is also known for its chemo preventive activity on multiple cancer conditions [16,42]. Similar to that, chemo preventive effect of ST03 was evident as it slowed down the proliferation of injected tumor cells. Pre and post-treatment with ST03 yielded better results than post-treatment alone. The delay in tumor cell proliferation observed in pretreated animals could be due to elevated levels of lymphocytes induced by ST03, which is under investigation. Thus, the effectiveness of ST03 at lower doses both in vitro and in vivo, makes it a better chemotherapeutic target than the parent compound. Also, lower concentrations of drugs might help in reducing off-target effects.

Conclusion

1,2-bis[(3E,5E)−3,5-bis[(2-chlorophenyl)methylene]−4-oxo-1-piperidyl]ethane-1,2-dione (ST03 regulates ROS production by altering mitochondrial membrane proteins and oxidative phosphorylation and induces cell. Owing to its bioavailability and stability than its parent compound curcumin, low doses of ST03 is effective against tumour growth with no apparent systemic toxicity.

Declaration of Competing Interest

Authors declare no conflict of interest.

CRediT authorship contribution statement

Jinsha Koroth: Conceptualization, Visualization, Formal analysis, Writing – original draft, Methodology. **Raghunandan Mahadeva:** Methodology. **Febina Ravindran:** Formal analysis, Writing – original draft, Methodology. **Tanvi R Parashar:** Methodology. **Vinay Teja:** Methodology, Methodology. **Subhas S Karki:** Resources. **Bibha Choudhary:** Conceptualization, Visualization, Formal analysis, Writing – original draft.

Supplementary materials

Supplementary material associated with this article can be found, in the online version, at doi:10.1016/j.tranon.2021.101280.

References

[1] F. Accurso, Curcumin and cystic fibrosis, J. Pediatr. Gastroenterol. Nutr. 39 (2004) 235.

[2] B.B. Aggarwal, A. Kumar, A.C. Bharti, Anticancer potential of curcumin: preclinical and clinical studies, Anticancer Res. 23 (2003) 363–398.

[3] H.P. Ammon, M.A. Wahl, Pharmacology of curcuma longa, Planta Med. 57 (1991) 1–7.

[4] P. Anand, A.B. Kunnumakkara, R.A. Newman, B.B. Aggarwal, Bioavailability of curcumin: problems and promises, Mol. Pharm. (2007), https://doi.org/10.1021/mp700113r.

[5] P. Anand, C. Sundaram, S. Jhurani, A.B. Kunnumakkara, B.B. Aggarwal, Curcumin and cancer: an "old-age" disease with an "age-old" solution, Cancer Lett. (2008), https://doi.org/10.1016/j.canlet.2008.03.025.

[6] R.J. Anto, A. Mukhopadhyay, K. Denning, B.B. Aggarwal, Curcumin (diferuloylmethane) induces apoptosis through activation of caspase-8, BID cleavage and cytochrome c release: its suppression by ectopic expression of Bcl-2 and Bcl-xl, Carcinogenesis 23 (2002) 143–150.

[7] T. Atsumi, K. Tonosaki, S. Fujisawa, Induction of early apoptosis and ROS-generation activity in human gingival fibroblasts (HGF) and human submandibular gland carcinoma (HSG) cells treated with curcumin, Arch. Oral Biol. 51 (2006) 913–921.

[8] N. Bilandzic, S. Terzic, B. Simic, Immunoglobulin changes in boars exposed to administration of levamisole and exogenous adrenocorticotropic hormone, Acta Vet. (2012), https://doi.org/10.2298/avb1206495b.

[9] S. Bleicken, M. Classen, P.V.L. Padmavathi, T. Ishikawa, K. Zeth, H.J. Steinhoff, E. Bordignon, Molecular details of Bax activation, oligomerization, and membrane insertion, J. Biol. Chem. 285 (2010) 6636–6647.

[10] E. Burgos-Morón, J.M. Calderón-Montaño, J. Salvador, A. Robles, M. López-Lázaro, The dark side of curcumin, Int. J. Cancer 126 (2010) 1771–1775.

[11] J. Cathcart, A. Pulkoski-Gross, J. Cao, Targeting matrix metalloproteinases in cancer: bringing new life to old ideas, Genes Dis. 2 (2015) 26–34.

[12] S. Das, U. Das, H. Sakagami, N. Umemura, S. Iwamoto, T. Matsuta, M. Kawase, J. Molnár, J. Serly, D.K.J. Gorecki, J.R. Dimmock, Dimeric 3,5-bis(benzylidene)-4-piperidones: a novel cluster of tumour-selective cytotoxins possessing multidrug-resistant properties, Eur. J. Med. Chem. 51 (2012) 193–199.

[13] U. Das, R.K. Sharma, J.R. Dimmock, 1,5-diaryl-3-oxo-1,4-pentadienes: a case for antineoplastics with multiple targets, Curr. Med. Chem. 16 (2009) 2001–2020.

[14] R.M.C. Di Martino, A. Bisi, A. Rampa, S. Gobbi, F. Belluti, Recent progress on curcumin-based therapeutics: a patent review (2012-2016). Part II: curcumin derivatives in cancer and neurodegeneration, Expert Opin. Ther. Pat. 27 (2017) 953–965.

[15] A.R. D'Souza, M. Minczuk, Mitochondrial transcription and translation: overview, Essays Biochem. 62 (2018) 309–320.

[16] A. Duvoix, R. Blasius, S. Delhalle, M. Schnekenburger, F. Morceau, E. Henry, M. Dicato, M. Diederich, Chemopreventive and therapeutic effects of curcumin, Cancer Lett. 223 (2005) 181–190.

[17] J. Epstein, I.R. Sanderson, T.T. Macdonald, Curcumin as a therapeutic agent: the evidence from in vitro, animal and human studies, Br. J. Nutr. 103 (2010) 1545–1557.

[18] R.R. Falah, W.H. Talib, S.J. Shbailat, Combination of metformin and curcumin targets breast cancer in mice by angiogenesis inhibition, immune system modulation and induction of p53 independent apoptosis, Ther. Adv. Med. Oncol. 9 (2017) 235–252.

[19] B. Farhangi, A.M. Alizadeh, H. Khodayari, S. Khodayari, M.J. Dehghan, V. Khori, A. Heidarzadeh, M. Khaniki, M. Sadeghiezadeh, F. Najafi, Protective effects of dendrosomal curcumin on an animal metastatic breast tumor, Eur. J. Pharmacol. (2015), https://doi.org/10.1016/j.ejphar.2015.03.076.

[20] C. Garrido, L. Galluzzi, M. Brunet, P.E. Puig, C. Didelot, G. Kroemer, Mechanisms of cytochrome c release from mitochondria, Cell Death Differ. (2006), https://doi.org/10.1038/sj.cdd.4401950.

[21] P. Ghosh, C. Vidal, S. Dey, L. Zhang, Mitochondria targeting as an effective strategy for cancer therapy, Int. J. Mol. Sci. 21 (2020), https://doi.org/10.3390/ijms21093363.

[22] S.C. Gupta, S. Prasad, J.H. Kim, S. Patchva, L.J. Webb, I.K. Priyadarsini, B. B. Aggarwal, Multitargeting by curcumin as revealed by molecular interaction studies, Nat. Prod. Rep. 28 (2011) 1937–1955.

[23] H. Hatcher, R. Planalp, J. Cho, F.M. Torti, S.V. Torti, Curcumin: from ancient medicine to current clinical trials, Cell. Mol. Life Sci. 65 (2008) 1631–1652.

[24] B. Hazra, B. Kumar, S. Biswas, B.N. Pandey, K.P. Mishra, Enhancement of the tumour inhibitory activity, in vivo, of diospyrin, a plant-derived quinonoid, through liposomal encapsulation, Toxicol. Lett. (2005), https://doi.org/10.1016/j.toxlet.2005.01.016.

[25] M. Hegde, S.S. Karki, E. Thomas, S. Kumar, K. Panjamurthy, S.R. Ranganatha, K. S. Rangappa, B. Choudhary, S.C. Raghavan, Novel levamisole derivative induces extrinsic pathway of apoptosis in cancer cells and inhibits tumor progression in mice, PLoS One 7 (2012) e43632.

[26] E.S. Helton, E. Scott Helton, X. Chen, p53 modulation of the DNA damage response, J. Cell. Biochem. (2007), https://doi.org/10.1002/jcb.21091.

[27] Y. He, Y. Yue, X. Zheng, K. Zhang, S. Chen, Z. Du, Curcumin, inflammation, and chronic diseases: how are they linked? Molecules 20 (2015) 9183–9213.

[28] C. Hu, M. Li, T. Guo, S. Wang, W. Huang, K. Yang, Z. Liao, J. Wang, F. Zhang, H. Wang, Anti-metastasis activity of curcumin against breast cancer via the inhibition of stem cell-like properties and EMT, Phytomedicine 58 (2019), 152740.

[29] A. Jabłońska-Trypuć, M. Matejczyk, S. Rosochacki, Matrix metalloproteinases (MMPs), the main extracellular matrix (ECM) enzymes in collagen degradation, as a target for anticancer drugs, J. Enzyme Inhib. Med. Chem. 31 (2016) 177–183.

[30] J. Koroth, S. Nirgude, S. Tiwari, V. Gopalakrishnan, R. Mahadeva, S. Kumar, S. S. Karki, B. Choudhary, Investigation of anti-cancer and migrastatic properties of novel curcumin derivatives on breast and ovarian cancer cell lines, BMC Complement. Altern. Med. 19 (2019) 273.

[31] D. Kumar, M. Kumar, C. Saravanan, S.K. Singh, Curcumin: a potential candidate for matrix metalloproteinase inhibitors, Expert Opin. Ther. Targets 16 (2012) 959–972.

[32] C.D. Lao, M.T. Ruffin, D. Normolle, D.D. Heath, S.I. Murray, J.M. Bailey, M. E. Boggs, J. Crowell, C.L. Rock, D.E. Brenner, Dose escalation of a curcuminoid formulation, BMC Complement. Altern. Med. (2006), https://doi.org/10.1186/1472-6882-6-10.

[33] J. Li, J. Zhang, J. Chen, X. Luo, W. Zhu, J. Shen, H. Liu, X. Shen, H. Jiang, Strategy for discovering chemical inhibitors of human cyclophilin a: focused library design, virtual screening, chemical synthesis and bioassay, J. Comb. Chem. 8 (2006) 326–337.

[34] G.Y. Liou, P. Storz, Reactive oxygen species in cancer, Free Radic. Res. 44 (2010) 479–496.

[35] W.D. Lu, Y. Qin, C. Yang, L. Li, Z.X. Fu, Effect of curcumin on human colon cancer multidrug resistance in vitro and in vivo, Clinics 68 (2013) 694–701.

[36] M.B. Maxwell, K.E. Maher, Chemotherapy-induced myelosuppression, Semin. Oncol. Nurs. 8 (1992) 113–123.

[37] S. Mishra, U. Narain, R. Mishra, K. Misra, Design, development and synthesis of mixed bioconjugates of piperic acid-glycine, curcumin-glycine/alanine and

[38] curcumin-glycine-piperic acid and their antibacterial and antifungal properties, Bioorg. Med. Chem. 13 (2005) 1477–1486.

[38] S. Mishra, K. Palanivelu, The effect of curcumin (turmeric) on Alzheimer's disease: an overview, Ann. Indian Acad. Neurol. 11 (2008) 13–19.

[39] S. Mondal, S. Bandyopadhyay, M.K. Ghosh, S. Mukhopadhyay, S. Roy, C. Mandal, Natural products: promising resources for cancer drug discovery, Anticancer Agents Med. Chem. 12 (2012) 49–75.

[40] D.O. Moon, M.O. Kim, Y.H. Choi, Y.M. Park, G.Y. Kim, Curcumin attenuates inflammatory response in IL-1beta-induced human synovial fibroblasts and collagen-induced arthritis in mouse model, Int. Immunopharmacol. 10 (2010) 605–610.

[41] K. Nagahama, T. Utsumi, T. Kumano, S. Maekawa, N. Oyama, J. Kawakami, Discovery of a new function of curcumin which enhances its anticancer therapeutic potency, Sci. Rep. 6 (2016) 787.

[42] G.P. Nagaraju, S. Aliya, S.F. Zafar, R. Basha, R. Diaz, B.F. El-Rayes, The impact of curcumin on breast cancer, Integr. Biol. (2012), https://doi.org/10.1039/c2ib20088k.

[43] S.O. Olusi, W.J. Jessop, A. Shoroye, Effects of levamisole on the immune responses of experimentally malnourished rats, Pediatr. Res. 13 (1979) 1237–1239.

[44] G. Padmanaban, P.N. Rangarajan, Curcumin as an adjunct drug for infectious diseases, Trends Pharmacol. Sci. 37 (2016) 1–3.

[45] S. Quintero-Fabián, R. Arreola, E. Becerril-Villanueva, J.C. Torres-Romero, V. Arana-Argáez, J. Lara-Riegos, M.A. Ramírez-Camacho, M.E. Alvarez-Sánchez, Role of matrix metalloproteinases in angiogenesis and cancer, Front. Oncol. 9 (2019) 1370.

[46] P.D. Ray, B.W. Huang, Y. Tsuji, Reactive oxygen species (ROS) homeostasis and redox regulation in cellular signaling, Cell Signal (2012), https://doi.org/10.1016/j.cellsig.2012.01.008.

[47] C.A. Reddy, V. Somepalli, T. Golakoti, A.K. Kanugula, S. Karnewar, K. Rajendiran, N. Vasagiri, S. Prabhakar, P. Kuppusamy, S. Kotamraju, V.K. Kutala, Mitochondrial-targeted curcuminoids: a strategy to enhance bioavailability and anticancer efficacy of curcumin, PLoS One 9 (2014) e89351.

[48] G. Sa, T. Das, Anti cancer effects of curcumin: cycle of life and death, Cell Div. 3 (2008) 14.

[49] S. Salvioli, A. Ardizzoni, C. Franceschi, A. Cossarizza, JC-1, but not DiOC 6 (3) or rhodamine 123, is a reliable fluorescent probe to assess Δ Ψ changes in intact cells: implications for studies on mitochondrial functionality during apoptosis, FEBS Lett. 411 (1997) 77–82.

[50] Y. Santiago-Vazquez, S. Das, U. Das, E. Robles-Escajeda, N.M. Ortega, C. Lema, A. Varela-Ramírez, R.J. Aguilera, J. Balzarini, E. De Clercq, S.G. Dimmock, D.K. J. Gorecki, J.R. Dimmock, Novel 3,5-bis(arylidene)-4-oxo-1-piperidinyl dimers: structure-activity relationships and potent antileukemic and antilymphoma cytotoxicity, Eur. J. Med. Chem. 77 (2014) 315–322.

[51] M. Schieber, N.S. Chandel, ROS function in redox signaling and oxidative stress, Curr. Biol. 24 (2014) R453–R462.

[52] M.K. Shanmugam, G. Rane, M.M. Kanchi, F. Arfuso, A. Chinnathambi, M.E. Zayed, S.A. Alharbi, B.K.H. Tan, A.P. Kumar, G. Sethi, The multifaceted role of curcumin in cancer prevention and treatment, Molecules 20 (2015) 2728–2769.

[53] R.L. Siegel, K.D. Miller, A. Jemal, Cancer statistics, 2019, CA Cancer J. Clin. 69 (2019) 7–34.

[54] E.P.de Siqueira, E.P. de Siqueira, J.P. Ramos, Chamaecostus subsessilis and Chamaecostus Cuspidatus (Nees & Mart) C. Specht and D.W. Stev as potential sources of anticancer agents, Nat. Prod. Chem. Res. (2016), https://doi.org/10.4172/2329-6836.1000204.

[55] F. Sivandzade, A. Bhalerao, L. Cucullo, Analysis of the mitochondrial membrane potential using the cationic JC-1 dye as a sensitive fluorescent probe, Bio-Protocol (2019), https://doi.org/10.21769/bioprotoc.3128.

[56] E.-.M. Strasser, B. Wessner, N. Manhart, E. Roth, The relationship between the anti-inflammatory effects of curcumin and cellular glutathione content in myelomonocytic cells, Biochem. Pharmacol. 70 (2005) 552–559.

[57] R.L. Thangapazham, A. Sharma, R.K. Maheshwari, Multiple molecular targets in cancer chemoprevention by curcumin, AAPS J. 8 (2006) E443–E449.

[58] D. Trachootham, J. Alexandre, P. Huang, Targeting cancer cells by ROS-mediated mechanisms: a radical therapeutic approach? Nat. Rev. Drug Discov. 8 (2009) 579–591.

[59] A. Vogel, J. Pelletier, Examen chimique de la racine de curcuma, J. Pharm. 1 (1815) 289–300.

[60] A. Vyas, P. Dandawate, S. Padhye, A. Ahmad, F. Sarkar, Perspectives on new synthetic curcumin analogs and their potential anticancer properties, Curr. Pharm. Des. 19 (2013) 2047–2069.

[61] H. Wang, T.O. Khor, L. Shu, Z.Y. Su, F. Fuentes, J.H. Lee, A.N.T. Kong, Plants vs. cancer: a review on natural phytochemicals in preventing and treating cancers and their druggability, Anticancer Agents Med. Chem. 12 (2012) 1281–1305.

[62] J. Wang, J. Yi, Cancer cell killing via ROS: to increase or decrease, that is the question, Cancer Biol. Ther. 7 (2008) 1875–1884.

[63] H. Yang, R.M. Villani, H. Wang, M.J. Simpson, M.S. Roberts, M. Tang, X. Liang, The role of cellular reactive oxygen species in cancer chemotherapy, J. Exp. Clin. Cancer Res. 37 (2018), https://doi.org/10.1186/s13046-018-0909-x.

[64] C. Yokoyama, Y. Sueyoshi, M. Ema, Y. Mori, K. Takaishi, H. Hisatomi, Induction of oxidative stress by anticancer drugs in the presence and absence of cells, Oncol. Lett. 14 (2017) 6066–6070.

[65] Y. Yuan, Y.S. Ju, Y. Kim, J. Li, Y. Wang, C.J. Yoon, Y. Yang, I. Martincorena, C. J. Creighton, J.N. Weinstein, Y. Xu, L. Han, H.L. Kim, H. Nakagawa, K. Park, P. J. Campbell, H. Liang, PCAWG Consortium, Author correction: comprehensive molecular characterization of mitochondrial genomes in human cancers, Nat. Genet. (2020), https://doi.org/10.1038/s41588-020-0629-y.

[66] R.-.Z. Zhao, S. Jiang, L. Zhang, Z.-.B. Yu, Mitochondrial electron transport chain, ROS generation and uncoupling (Review), Int. J. Mol. Med. 44 (2019) 3–15.

[67] L.D. Zheng, Q.S. Tong, C.H. Wu, Growth inhibition and apoptosis inducing mechanisms of curcumin on human ovarian cancer cell line A2780, Chin. J. Integr. Med. 12 (2006) 126–131.

[68] H. Zhou, C.S. Beevers, S. Huang, The targets of curcumin, Curr. Drug Targets 12 (2011) 332–347.

[69] M.D. Kendall, Functional histology: A text and colour atlas, J. Anatomy 130 (Pt 3) (1980) 633.